

# Journal of Materials Chemistry A

Accepted Manuscript

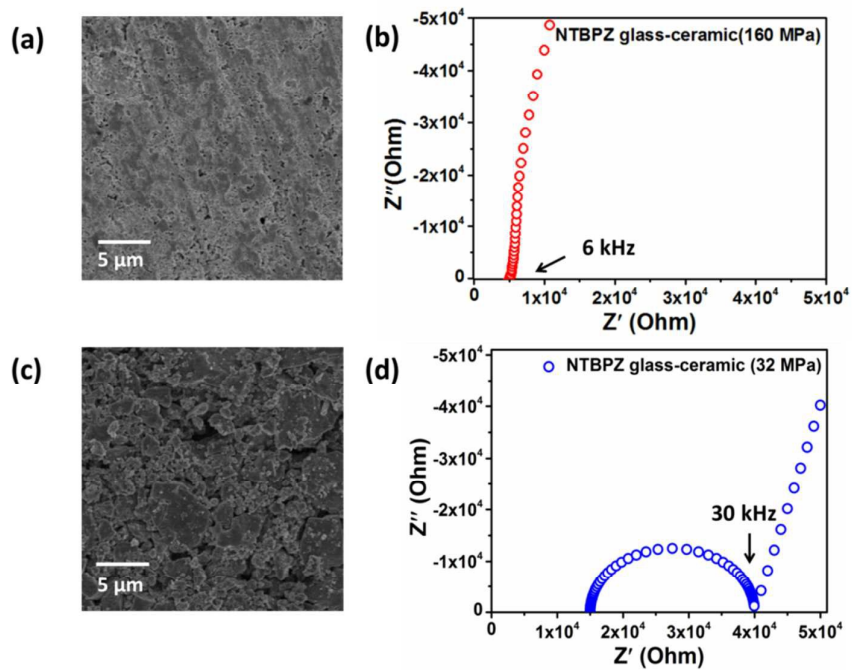


This is an *Accepted Manuscript*, which has been through the Royal Society of Chemistry peer review process and has been accepted for publication.

*Accepted Manuscripts* are published online shortly after acceptance, before technical editing, formatting and proof reading. Using this free service, authors can make their results available to the community, in citable form, before we publish the edited article. We will replace this *Accepted Manuscript* with the edited and formatted *Advance Article* as soon as it is available.

You can find more information about *Accepted Manuscripts* in the [Information for Authors](#).

Please note that technical editing may introduce minor changes to the text and/or graphics, which may alter content. The journal's standard [Terms & Conditions](#) and the [Ethical guidelines](#) still apply. In no event shall the Royal Society of Chemistry be held responsible for any errors or omissions in this *Accepted Manuscript* or any consequences arising from the use of any information it contains.



A new type fluorophosphate ( $\text{Na}_2\text{O}+\text{NaF}$ )- $\text{TiO}_2$ - $\text{B}_2\text{O}_3$ - $\text{P}_2\text{O}_5$ - $\text{ZrF}_4$  (NTBPZ) glass and glass-ceramic by heat treatment have a sodium-ion conductivity up to  $7 \times 10^{-9} \text{ S} \cdot \text{cm}^{-1}$  and  $3 \times 10^{-5} \text{ S} \cdot \text{cm}^{-1}$ , respectively. The improvement of sodium-ion conductivity due to conductive phase  $\text{NaTi}_2(\text{PO}_4)_3$  form and the grain boundary resistance decrease by cold pressing.



Journal Name

COMMUNICATION

## A Fluorophosphate Glass-ceramic Electrolyte with Superior Ionic Conductivity and Stability for Na-ion Batteries†

Received 00th January 20xx,  
Accepted 00th January 20xx

DOI: 10.1039/x0xx00000x

www.rsc.org/

Yiwen Ni †, Ruilin Zheng †, Xiaowen Tan, Weiyan Yue, Peng Lv, Jie Yang, Dan Song, Kehan Yu \* and Wei Wei \*

† These authors contributed equally.

All solid-state sodium-ion electrolytes have attracted increasing attention due to their wide range of applications in secondary batteries. Here, a new fluorophosphate glass-ceramic electrolyte, (Na<sub>2</sub>O+NaF)-TiO<sub>2</sub>-B<sub>2</sub>O<sub>3</sub>-P<sub>2</sub>O<sub>5</sub>-ZrF<sub>4</sub> (NTBPZ), was proposed and synthesized. Due to a low activation energy of 13.9 kJ·mol<sup>-1</sup> and reduced resistance at the grain boundaries, the NTBPZ glass ceramic has a room-temperature ionic conductivity as high as 3×10<sup>-5</sup> S·cm<sup>-1</sup>. In addition, the NTBPZ electrolyte has excellent thermal and chemical stabilities in ambient condition. These outstanding performances make the NTBPZ a promising electrolyte for all-solid-state sodium-ion batteries.

Increasing demand for large scale secondary batteries with high energy densities has been accelerated by fast spreading electric vehicles and distributed power systems at individual houses.<sup>1-4</sup> The rechargeable all-solid-state sodium-ion batteries have attracted increasing attention in the application of large-scale energy storage due to the abundant sodium sources.<sup>3-6</sup> The safety and cost issues of the organic liquid electrolytes have stimulated the development of all-solid-state sodium-ion batteries.<sup>7-9</sup>

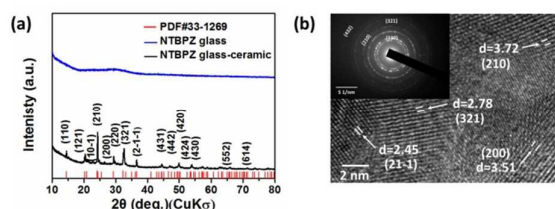
In the literature, chalcogenide glass and glass-ceramic electrolytes with high ionic conductivities have been extensively studied for the room-temperature sodium-ion batteries. Since the discovery of sulphide glass electrolytes in 1980, significant advances have been witnessed by some representative glasses, such as Na<sub>2</sub>S-SiS<sub>2</sub> and Na<sub>2</sub>(Ga<sub>0.1</sub>Ge<sub>0.9</sub>)<sub>2</sub>Se<sub>4.95</sub> with room-temperature ionic conductivity up to 10<sup>-5</sup> S·cm<sup>-1</sup>.<sup>10,11</sup> Most recently, Hayashi et al. reported a cubic Na<sub>3</sub>PS<sub>4</sub> glass-ceramic with a record high ionic conductivity of 3×10<sup>-4</sup> S·cm<sup>-1</sup> at room temperature.<sup>6</sup> Nevertheless, suffering from high cost of the raw materials and poor ambient stability, the chalcogenide glass and glass-ceramic electrolytes are far from practical uses.<sup>12-16</sup>

In contrast, oxide glass and glass-ceramic electrolytes have much

better chemical stability, simple preparation processes, and easy availability and low cost of the raw materials.<sup>17-19</sup> Moreover, the room-temperature ionic conductivities have been demonstrated for the sodium oxide glasses such as Na<sub>2</sub>O-SiO<sub>2</sub>, P<sub>2</sub>O<sub>5</sub>-FeO-Na<sub>2</sub>O, and P<sub>2</sub>O<sub>5</sub>-B<sub>2</sub>O<sub>3</sub>-Na<sub>2</sub>O with 1×10<sup>-7</sup> S·cm<sup>-1</sup>, 5×10<sup>-7</sup> S·cm<sup>-1</sup>, and 10<sup>-9</sup> S·cm<sup>-1</sup>, respectively.<sup>20-22</sup> The relatively low conductivities are partially resulted from high activation energies and grain boundaries.<sup>23</sup> Comparing with the glass-ceramic electrolytes, in the same system the pure glass and pure ceramic electrolytes have the largest grain resistance and interparticle resistance, respectively.

In this study, we developed a stable glass-ceramic, which is a high-temperature phase converted from the fluorophosphate (Na<sub>2</sub>O+NaF)-TiO<sub>2</sub>-B<sub>2</sub>O<sub>3</sub>-P<sub>2</sub>O<sub>5</sub>-ZrF<sub>4</sub> (NTBPZ) glass. The starting material, P<sub>2</sub>O<sub>5</sub>-B<sub>2</sub>O<sub>3</sub>-Na<sub>2</sub>O (NBP) system, has a large temperature range of glass formation. Then an addition of certain amount of ZrF<sub>4</sub> and TiO<sub>2</sub> plays a role of nucleating agent. Meanwhile, the NaF inhibits fast crystallization during the cooling of the glass. Overall, the NTBPZ glass-ceramic is feasible to make.

A room-temperature ionic conductivity of 3×10<sup>-5</sup> S·cm<sup>-1</sup> and a low conduction activation energy (*E<sub>a</sub>*) of 13.9 kJ·mol<sup>-1</sup> were obtained for the NTBPZ glass-ceramic electrolyte. The conductive phase, NaTi<sub>2</sub>(PO<sub>4</sub>)<sub>3</sub> nanocrystals, provided spacious conductive channels for the sodium ions. Plenty of defects in the NaTi<sub>2</sub>(PO<sub>4</sub>)<sub>3</sub> nanocrystals in the NTBPZ glass-ceramic lowered the activation energy. The grain boundary resistance of the NTBPZ electrolyte was reduced by heat treatment and cold-pressing processes. The relationship between the sodium-ion conductivity and the grain boundary resistance was discussed. Compared with the chalcogenide glass-ceramic electrolytes, the NTBPZ glass-ceramic is prepared using simpler processes and cheaper raw materials, and thus is promising for the large-scale application.



School of Optoelectronic Engineering and Institute of Advanced Materials,  
Nanjing University of Posts & Telecommunications, Nanjing 210023, China  
E-mail: kehanyu@njupt.edu.cn, weiwei@njupt.edu.cn;

†Electronic Supplementary Information (ESI) available See  
DOI: 10.1039/x0xx00000x

**Fig. 1** (a) XRD patterns of NTBPPZ glass and  $\text{NaTi}_2(\text{PO}_4)_3$  crystal in the NTBPPZ glass-ceramic. (b) HRTEM image and diffraction ring of  $\text{NaTi}_2(\text{PO}_4)_3$  nanocrystals in the NTBPPZ glass-ceramic.

In order to obtain a homogenous NTBPPZ glass-ceramic conductor, the NTBPPZ glass powder was heated above the crystallization temperature ( $T_c$ ). When the temperature exceeded the glass transition temperature ( $T_g$ ), the glass particles were fused into a dense unity which was subsequently transformed into a glass-ceramic by further heat treatment above the  $T_c$ .

The  $T_g$  at 451 °C and the  $T_c$  at 485 °C were determined by the differential scanning calorimetry (DSC) while the exothermic crystallization ended at 650 °C (Fig. S1). In order to control the size of the  $\text{NaTi}_2(\text{PO}_4)_3$  nanocrystals, the heat treatment temperature was set at 515 °C. As shown in the Fig. S2, the ionic conductivity was decreased if the heat-treat temperature was below or above 515 °C. After the heat treatment, part of NTBPPZ glass phase was transformed into  $\text{NaTi}_2(\text{PO}_4)_3$  nanocrystals. Fig. 1a shows the X-ray diffraction (XRD) patterns of the NTBPPZ glass and glass-ceramic. The  $\text{NaTi}_2(\text{PO}_4)_3$  crystal is R-3c type according to previous reports.<sup>30,31</sup> The transmission electron microscope (TEM) image clearly shows the nanocrystals embedded in the glass matrix (Fig. 1b). The lattice constants and corresponding (210), (321), (21-1), and (200) planes are marked in the Fig. 1b. The electron diffraction pattern of the  $\text{NaTi}_2(\text{PO}_4)_3$  is shown in the inset of the Fig. 1b.

In the sodium oxide glass, the network connections of glass structure is consisted of the oxygen ions with covalent bonds, only little sodium ions can move in the network, leading to low ionic conductivity.<sup>32-34</sup> But some defects formed during the crystallization lowered the activation energy ( $E_a$ ). The unit-cell of the  $\text{NaTi}_2(\text{PO}_4)_3$  trigonal structure consists of  $\text{TiO}_6$  (octahedron) and  $\text{PO}_4$  (tetrahedron) (Fig. 2a). The size of the channels for the  $\text{Na}^+$  becomes greater (102Å) with the existence of Ti-O and P-O (Fig. 2b). The ionic conductivity is improved significantly due to the R-3c (167) space-group of the  $\text{NaTi}_2(\text{PO}_4)_3$  that opens wide clearance for  $\text{Na}^+$  transmission.

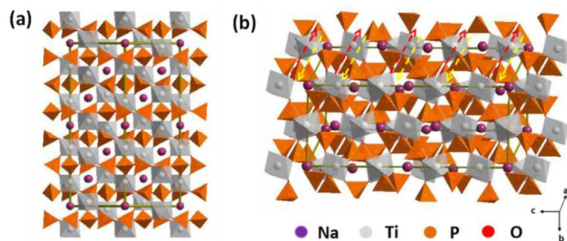


**Fig. 2** (a) Crystal structure of  $\text{NaTi}_2(\text{PO}_4)_3$  and (b) channel network of sodium-ion conduction pathways in NTBPPZ glass-ceramic.

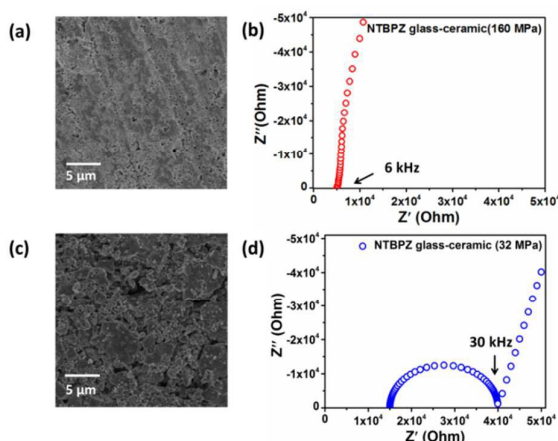


**Fig. 3** SEM images of NTBPPZ glass-ceramic sample after cold pressing at (a) 160 MPa and (c) 32 MPa at 25 °C. Nyquist plots of the NTBPPZ glass-ceramic impedances at (b) 160 MPa and (d) 32 MPa at 25 °C.

The alternating current (AC) impedance measurements were employed to evaluate the conductivities of the NTBPPZ glass and the glass-ceramic. While the cold-press method moulds the glass-ceramic powder into a dense pellet, the grain boundaries could hardly be eliminated. The AC impedance spectra are clearly separated into the cold-pressed NTBPPZ glass and NTBPPZ glass-ceramic at 32 MPa (Fig. S3). The Nyquist plot of the impedance spectrum of the NTBPPZ glass pellet exhibits a big semicircle at high frequency and a slope at the low-frequency region which are due to bulk and grain boundary responses together. In contrast, the impedance spectrum of the pellet of the NTBPPZ glass-ceramic prepared by heat treatment at 515 °C exhibited a smaller semicircle, and the resistance of the pellet decreased. The sodium-ion conductivities at 25 °C of the cold-pressed NTBPPZ glass and glass-ceramic at 32 MPa are  $2 \times 10^{-9} \text{ S}\cdot\text{cm}^{-1}$  and  $5 \times 10^{-6} \text{ S}\cdot\text{cm}^{-1}$ , respectively. Compared with the NTBPPZ glass, this difference is attributable to the formation of  $\text{NaTi}_2(\text{PO}_4)_3$  nanocrystals (Fig. S4). While the total number of defects fitting the conductive ions formed by  $\text{NaTi}_2(\text{PO}_4)_3$  nanocrystals are more than conductible ions, the energy of movable ions will be regarded as a part of energy which provide for the conductive ions transmitting in the NTBPPZ glass-ceramic, it would be equal to approximately lattice energy.<sup>35-37</sup>

Although grain boundary resistance of the NTBPPZ glass-ceramic (32 MPa) has reduced more than the NTBPPZ glass (32 MPa) (Fig. 3d), the all boundary (bulk and grain) of the NTBPPZ glass-ceramic still remained a large grain boundary resistance. The impedance spectra are clearly semicircle only in low pressure. When the pressure increases from 32 MPa to 160 MPa, the semicircle at low frequencies of the glass-ceramic disappears, and the sodium-ion conductivity is up to  $3 \times 10^{-5} \text{ S}\cdot\text{cm}^{-1}$  (Fig. 3b). The Bode plots at 25 °C of the pellets of the NTBPPZ after cold pressing glass-ceramic at 160 MPa and 32 MPa are showed in Fig. S5. The disappearance of the semicircle suggests the contribution of the grain boundary to the total resistance in the NTBPPZ glass-ceramic by the given pressure improved, which can be expected from the grain boundaries in the SEM image (Fig. 3a, 3c).

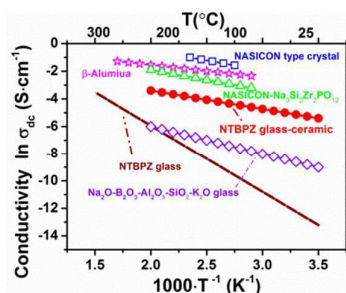


**Fig. 4** Conductivity of the Arrhenius plots of the NTBPZ glass, NTBPZ glass-ceramic and several sodium-ion conductors reported so far are also shown as a comparison.

It can be showed in Fig. 3a, c that the cold-compress pressure dependency of the bulk and grain boundary contributions in glass-ceramic material at room temperature. On the other hand, temperature dependencies of the ionic conductivities can be showed in Fig. S2. The results showed that heat-treat temperature and holding time are two important factors affecting the grain size and uniformity, then affected the sodium-ion conductivity.

The ionic conductivity of some typical solid sodium-ion electrolytes and NTBPZ glass and glass-ceramic electrolytes are plotted in Fig. 4. The activation energies ( $E_a$ ) of the NTBPZ glass and the NTBPZ glass-ceramic are  $58.75 \text{ kJ}\cdot\text{mol}^{-1}$  and  $13.64 \text{ kJ}\cdot\text{mol}^{-1}$ , respectively, calculated by fitting the data to the Arrhenius equation.<sup>38</sup> The NTBPZ glass pellet (open circles) has the best conductivity of  $7 \times 10^{-9} \text{ S}\cdot\text{cm}^{-1}$  at room-temperature. Such differences would be expected to build dependence between non-Arrhenius temperature and ionic conductivity, where the lower active energy can get higher ionic conductivity. It can be shown that as the average value of the energy distribution changes with changing glass or glass-ceramic composition to higher and lower values, these temperature ranges would in turn change to higher and lower values, respectively. The evidence is consistent with the behaviour observed for nearly all oxide glasses studied in the literature to date, although some examples of non-Arrhenius behaviour do exist.<sup>39-41</sup> Moreover, in the more recent literature of the glasses with higher ionic conductivity (lower average activation energy), several instances of non-Arrhenius temperature dependence of the alkali ionic conductivity in sulphide glasses can be found.<sup>42-45</sup>

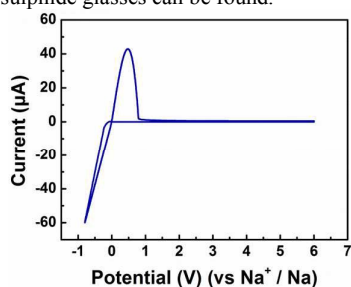


**Fig. 5** Cyclic voltammogram of the NTBPZ glass-ceramic electrolyte.

By the method of cyclic voltammogram, we measured the voltage window of the NTBPZ glass-ceramic electrolyte, as shown in Fig. 5. It suggests that the NTBPZ glass-ceramic electrolyte has a wide electrochemical window except an insignificant oxidation currents

observed from 0 V to 0.8 V, the reversible sodium deposition and dissolution of  $\text{Na}^+/\text{Na}$  currents take place from 1 V to 6 V. The counter/reference electrode measured is sodium foil and a stainless-steel disk as the working electrode. The potential sweep was tested by a scanning rate of  $5 \text{ mV}\cdot\text{s}^{-1}$  at room temperature.

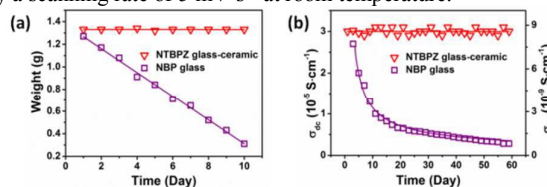


**Fig. 6** Sodium ionic conductivity of NTBPZ glass-ceramic and NBP glass in the air for two month (a), and chemical stability of NTBPZ glass-ceramic and NBP glass in the air for 10 days (b).

The sodium electrolytes can be realized in the sodium batteries needed high sodium-ion conductivity as well as excellent chemical stability. The sodium-ion conductivity of chalcogenide electrolytes can be decreased due to unimproved chemical stability. In this study, we put the samples in open air in order to track the relationship between the chemical stability and sodium-ion conductivity of the NTBPZ glass-ceramic and  $\text{Na}_2\text{O-B}_2\text{O}_3\text{-P}_2\text{O}_5$  glass<sup>30</sup> for ten days and two months, respectively.

It should be noted there is a significant difference in the chemical stability between NTBPZ glass-ceramic and NBP glass, which have a great impact on the sodium-ion conductivity. However, the NBP glass makes a reaction in the air and weathered (Fig. 6a). It can be observed that the NTBPZ glass-ceramic has a better chemical stability than the NBP glass. At the same time, the sodium-ion conductivity of the NBP glass and the NTBPZ glass-ceramic changed over time as shown in Fig. 6b. It can be proved that the sodium-ion conductivity of NTBPZ glass-ceramic remained unchanged basically, but the sodium-ion conductivity of NBP glass has been rapidly lower. This agreement suggests that the NTBPZ glass-ceramic can be used for a safety ionic electrolyte at room-temperature. Consequently, it can maintain stable high sodium-ion conductivity for long time.

## Conclusions

In summary, an  $(\text{Na}_2\text{O}+\text{NaF})\text{-TiO}_2\text{-B}_2\text{O}_3\text{-P}_2\text{O}_5\text{-ZrF}_4$  (NTBPZ) glass-ceramic electrolyte with an ionic conductivity up to  $3 \times 10^{-5} \text{ S}\cdot\text{cm}^{-1}$  at room temperature is realized for the first time. The conduction activation energy of this electrolyte is  $13.64 \text{ kJ}\cdot\text{mol}^{-1}$ . In addition, the NTBPZ glass-ceramic electrolyte has an excellent thermal stability below  $500 \text{ }^\circ\text{C}$  and chemical stability in the ambient condition. The electrolyte is made with low-cost raw materials and simple preparation processes.

## Experimental Section

NTBPZ ( $42(\text{Na}_2\text{O}+\text{NaF})\text{-}2\text{TiO}_2\text{-}13\text{B}_2\text{O}_3\text{-}38\text{P}_2\text{O}_5\text{-}5\text{ZrF}_4$ ) glass was prepared by a conventional melt-quenching method.  $\text{NaPO}_3$  (Aldrich, 99%),  $\text{TiO}_2$  (Aldrich, 99%),  $\text{H}_3\text{BO}_3$  (Alfa,

99.99%), P<sub>2</sub>O<sub>5</sub> (Aldrich, 99.99%), NaF (Aldrich, 99.99%) and ZrF<sub>4</sub> (Alfa, 99.9%) precursors were mixed in stoichiometric proportions, then melted in an alumina crucible in a globe electrical furnace at 1300-1350 °C for 40 min. The molten sample was rapidly quenched in liquid nitrogen to obtain the NTBZ glass. The NTBZ glass powders took preparation of the NTBZ glass by a mechanical method through planetary ball mill (QM-QX, QM-QX4). The NTBZ glass was placed into a zirconia (ZrO<sub>2</sub>) vessel (internal volume of 50 ml) with 40 ZrO<sub>2</sub> balls (4 mm in diameter). The process used rotation speed of 510 r.p.m. for 5 hours. Then, the NTBZ glass powders were heated at 515 °C for 15 hours to obtain the NTBZ glass-ceramic powders. Finally the NTBZ glass and glass-ceramic electrolyte powders were compressed by a cold pressed method to prepare a pellet that was 10 mm in diameter and 1 mm thick for electrical measurements.

The T<sub>c</sub> was determined by differential scanning calorimetry (PerkinElmer, STA 8000). XRD (D8 Advance, Bruker) measurements of the prepared materials were performed using Cu K $\alpha$  to identify the crystalline phases. Microstructure of cross-section for the electrolyte pellets was observed by SEM (S4800, Hitachi). Transmission electron microscope images of the diffraction ring were tested by TEM (2100F, JEM).

The electrical conductivities of the cold-pressed NTBZ glass and glass-ceramic powder samples were measured using an AC impedance method under Ar gas. The NTBZ glass and glass-ceramic were cold-compressed in 32 MPa and 160 MPa (MS1-100, RIKEN) separated into pellets with a 10 mm diameter, stainless steel plates were attached to both sides of the pellet as the electrodes. Impedance spectra were recorded using an impedance analyser (1470E, Solartron) in the frequency range between 1 Hz and 1 MHz

## Acknowledgements

This work was financially supported by the National Natural Science Foundation of China (Grant No. 61274054), NUPTSF (Grant No. NY214056, NY214137).

## Notes and references

- W. Li, J. Dahn and D. Wainwright, *Science*, 1994, 264, 1115-1118.
- P. G. Bruce, S. A. Freunberger, L. J. Hardwick and J.-M. Tarascon, *Nature materials*, 2012, 11, 19-29.
- H. D. Yoo, I. Shterenberg, Y. Gofer, G. Gershinsky, N. Pour and D. Aurbach, *Energy & Environmental Science*, 2013, 6, 2265-2279.
- J. B. Goodenough, *Accounts of chemical research*, 2012, 46, 1053-1061. M. Tatsumisago, M. Nagao and A. Hayashi, *Journal of Asian Ceramic Societies*, 2013, 1, 17-25.
- J.-M. Tarascon and M. Armand, *Nature*, 2001, 414, 359-367.
- N. Kamaya, K. Homma, Y. Yamakawa, M. Hirayama, R. Kanno, M. Yonemura, T. Kamiyama, Y. Kato, S. Hama and K. Kawamoto, *Nature Materials*, 2011, 10, 682-686.
- A. Hayashi, K. Noi, A. Sakuda and M. Tatsumisago, *Nature Communications*, 2012, 3, 856.
- H. Pan, Y.-S. Hu and L. Chen, *Energy & Environmental Science*, 2013, 6, 2338-2360.
- B. L. Ellis and L. F. Nazar, *Current Opinion in Solid State and Materials Science*, 2012, 16, 168-177.
- M. D. Slater, D. Kim, E. Lee and C. S. Johnson, *Advanced Functional Materials*, 2013, 23, 947-958.
- T. Kudo and J. Kawamura, *Materials for Energy Conversion Devices*, Woodhead Publishing, Cambridge, UK, 2005, 174-211.
- S. K. Kim, A. Mao, S. Sen and S. Kim, *Chemistry of Materials*, 2014, 26, 5695-5699.
- O. Bohnke, S. Ronchetti and D. Mazza, *Solid State Ionics*, 1999, 122, 127-136.
- S. Banerjee, J. M. Szarko, B. D. Yuhus, C. D. Malliakas, L. X. Chen and M. G. Kanatzidis, *Journal of the American Chemical Society*, 2010, 132, 5348-5350.
- M. Tatsumisago and A. Hayashi, *International Journal of Applied Glass Science*, 2014, 5, 226-235.
- J. H. Kennedy, Z. Zhang and H. Eckert, *Journal of Non-Crystalline Solids*, 1990, 123, 328-338.
- M. Ribes, B. Barrau and J. Souquet, *Journal of Non-Crystalline Solids*, 1980, 38, 271-276.
- S.-B. Sohn, S.-Y. Choi, G.-H. Kim, H.-S. Song and G.-D. Kim, *Journal of non-crystalline solids*, 2002, 297, 103-112.
- Hui Xia, Hai Long Wang, Wei Xiao, Man On Lai, Li Lu, *International Journal of Surface Science and Engineering*, 2009, 3, 23-43.
- M.-H. Yeh, C.-L. Sun, J.-S. Su, L.-Y. Lin, C.-P. Lee, C.-Y. Chen, C.-G. Wu, R. Vittal and K.-C. Ho, *Carbon*, 2012, 50, 4192-4202.
- K. Ngai and C. Moynihan, *Mrs Bulletin*, 1998, 23, 51-56.
- R. Christensen, J. Byer, T. Kaufmann and S. W. Martin, *Physics and Chemistry of Glasses-European Journal of Glass Science and Technology Part B-European Journal of Glass Science and Technology Part B*, 2009, 50, 237-242.
- D. Day, *Physics and Chemistry of Glasses-European Journal of Glass Science and Technology Part B*, 1999, 40, 69-74.
- R. Christensen, G. Olson and S. W. Martin, *The Journal of Physical Chemistry B*, 2013, 117, 2169-2179.
- W. Zhaoyin, *Shanghai Energy Conservation*, 2007, 2, 7-10.
- C.-W. Park, H.-S. Ryu, K.-W. Kim, J.-H. Ahn, J.-Y. Lee and H.-J. Ahn, *Journal of Power Sources*, 2007, 165, 450-454.
- C. Haering, A. Roosen, H. Schichl and M. Schnöller, *Solid State Ionics*, 2005, 176, 261-268.
- Q. Zhang, Z. Wen, Y. Liu, S. Song and X. Wu, *Journal of Alloys and Compounds*, 2009, 479, 494-499.
- A. Kapustinskii, *Q. Rev. Chem. Soc.*, 1956, 10, 283-294.
- B. Papke, M. Ratner and D. Shriver, *Journal of the Electrochemical Society*, 1982, 129, 1694-1701.
- D. MacFarlane, P. Meakin, J. Sun, N. Amini and M. Forsyth, *The Journal of Physical Chemistry B*, 1999, 103, 4164-4170.
- C. Delmas, A. Nadiri and J. Soubeyroux, *Solid State Ionics*, 1988, 28, 419-423.
- S. Murugavel, C. Vaid, V. Bhadrani and C. Narayana, *The Journal of Physical Chemistry B*, 2010, 114, 13381-13385.
- S. Murugavel, *Physical Review B*, 2005, 72, 134204.
- N. Kuwata, T. Saito, M. Tatsumisago, T. Minami and J.

## Journal Name

## COMMUNICATION

- Kawamura, *Solid state ionics*, 2004, 175, 679-682.
42. J. Kincs and S. W. Martin, *Physical Review Letters*, 1996, 76, 70.
43. B. Meyer, F. Borsa, D. M. Martin and S. W. Martin, *Physical Review B*, 2005, 72, 144301.
44. Q. Mei, B. Meyer, D. Martin and S. W. Martin, *Solid State Ionics*, 2004, 168, 75-85.
45. M. Ribes, G. Taillades and A. Pradel, *Solid State Ionics*, 1998, 105, 159-165.